

Structural and Oxo-Transfer Reactivity Differences of Hexacoordinate and Pentacoordinate (Nitro)(tetraphenylporphinato)cobalt(III) Derivatives

John Goodwin,^{*,†} Rosa Bailey,[‡] William Pennington,[‡] Roger Rasberry,[†] Tony Green,[†] Shira Shasho,[†] May Yongsavanh,[†] Valerie Echevarria,[†] Jessica Tiedeken,[†] Christina Brown,[†] George Fromm,[†] Stephanie Lyerly,[§] Natalie Watson,[§] Amy Long,[§] and Nick De Nitto[§]

Department of Chemistry and Physics, Coastal Carolina University, P.O. Box 261954, Conway, South Carolina 29526-6054, Department of Chemistry, Clemson University, Clemson, South Carolina 29634-1905, and The South Carolina Governor's School for Mathematics and Science, Hartsville, South Carolina 29550

Received December 22, 2000

The oxo-transfer catalyst (nitro)(pyridyl)cobalt(III) tetraphenylporphyrin has been reinvestigated by substitution of the distal pyridine ligand with 4-*N,N*-dimethylaminopyridine and 3,5-dichloropyridine. Differences in their structures and in the reactivity of the compounds toward catalytic secondary oxo transfer were investigated by FT-IR and UV–visible spectroscopy, cyclic voltammetry, X-ray diffraction, semiempirical calculations, and reactions with alkenes in dichloromethane solution. Very modest differences in the hexacoordinate compounds' structures were predicted and observed, but the secondary oxo-transfer reactivity at the nitro ligand varies markedly with the basicity of the pyridine ligand and the position of the coordination equilibrium. Oxo transfer occurs rapidly through the pentacoordinate species (nitro)cobalt(III) tetraphenylporphyrin that is generated by dissociation of the pyridine ligand and therefore is strongly related to the Hammett parameters of these nitrogenous bases. The reactive pentacoordinate species CoTPP(NO₂) can be generated in solution by addition of lithium perchlorate to (py)CoTPP(NO₂) by Lewis acid–base interactions or more simply by using the weaker Lewis base Cl₂py instead of py as the distal ligand. In contrast to pentacoordinate (nitro)iron porphyrins, disproportionation reactions of CoTPP(NO₂) compound are not evident. This pentacoordinate derivative, CoTPP(NO₂), is reactive enough to stoichiometrically oxidize allyl bromide in minutes. Preliminary catalytic oxidation reaction studies of alkenes also indicate the involvement of both radical and nonradical oxo-transfer steps in the mechanism, suggesting formation of a peroxynitro intermediate in the reaction of the reduced CoTPP(NO) with O₂.

Introduction

Secondary oxo-transfer reactions from metal-coordinated nitrite occur with formation of reduced metal nitrosyl complexes. In some of these reduced nitrosyl products, the NO ligand can then react with dioxygen to be oxidized back to the nitro ligand with concomitant reoxidation of the metal center. This reaction sequence has been an intriguing prospect for dioxygen activation and industrial oxo-transfer catalysis for over two decades.^{1,2} The advantages of this approach are primarily in avoiding radical mechanisms that reduce specificity of reaction and stability of the catalysts by autoxidation and secondly in the use of dioxygen as the ultimate oxidant rather than organic peroxides or hydrogen peroxide.

The complex (nitro)(pyridyl)(tetraphenylporphinato)cobalt(III), (py)Co^{III}TPP(NO₂), was studied² in detail and patented

for industrial catalysis in the late 1970s and early 1980s, and was promising because of its catalytic activity for a wide range of oxidation reactions. Several studies of this compound dealt with a variety of mechanisms corresponding to the range of reactions, and these were proposed to include bimolecular oxo transfer to activated olefins, intramolecular oxo-transfer reactions promoted by Lewis acids, and nitro exchange reactions.^{2,3} However, the catalyst had low turnover numbers and required cocatalysts for oxidation of alkenes. No systematic structural variations of the cobalt porphyrin compound for tuning its oxo-transfer reactivity or detailed examinations of the mechanism of Lewis acid activation have been presented. Now, through study of a series of derivatives of the parent compound that varied the basicity of the distal pyridine ligand, the importance of the Lewis acid in promoting dissociation of this distal pyridine ligand in oxo-transfer reactivity has been clarified. The pentacoordinate nitro complex has been found to be much more reactive than the hexacoordinate pyridyl analogues to the extent that this catalyst is for the first time able to promote dioxygen activation and oxidation of unactivated alkenes. Reactivity with alkenes indeed appears to be limited to this pentacoordinate species. This observation parallels a recent report of extreme oxo-transfer reactivity of pentacoordinate (nitro)iron(III) picket-fence porphyrin prepared in solution by Munroe and Scheidt.⁴

[†] Coastal Carolina University.

[‡] Clemson University.

[§] Students from The South Carolina Governor's School for Mathematics and Science.

- (1) Cotton, F. A.; Wilkinson, G. *Advanced Inorganic Chemistry*, 5th ed.; Wiley: New York, 1988; pp 1281–1282 and references therein.
- (2) (a) Tovrog, B. S.; Diamond, S. E.; Mares, F. *J. Am. Chem. Soc.* **1979**, *101*, 270–272. (b) Tovrog, B. S.; Mares, F.; Diamond, S. E. *J. Am. Chem. Soc.* **1980**, *102*, 6616–6618. (c) Tovrog, B. S.; Diamond, S. E.; Mares, F.; Stalkiewicz, A. *J. Am. Chem. Soc.* **1981**, *103*, 3522–3526. (d) Diamond, S. E.; Mares, F.; Szalkiewicz, A.; Muccigrosso, D. A.; Solar, J. P. *J. Am. Chem. Soc.* **1982**, *104*, 4266–4268. (e) Ercolani, C.; Paoletti, A. M.; Pennesi, G.; Rossi, G. *J. Chem. Soc., Dalton Trans.* **1991**, 1317–21.

- (3) Andrews, M. A.; Chang, C.-T.; Cheng, C.-W. *Organometallics* **1985**, *4*, 268–274.

However, unlike the observations for the iron derivative, this pentacoordinate (nitro)cobalt system is apparently stable with respect to disproportionation reactions.

Experimental Section.

General Methods. Spectroscopic Methods. Infrared spectra were recorded as KBr disks using a Bomem Michelson FT-IR system. Solution UV-visible spectra were recorded under nitrogen atmosphere using screw-capped 1-cm path length cells with a Hewlett-Packard 8453 diode array spectrometer or in a Vacuum-Atmospheres Glovebox with an Ocean Optics PC1000 fiber optics spectrometer controlled by OOIBASE 1.5 or OOIBASE32 operating software. Reflectance spectra of porphyrins adsorbed on silica gel were collected with the fiber optics spectrometer using an Ocean Optics reflectance probe. Proton NMR spectra were recorded in CDCl_3 or CD_2Cl_2 (Aldrich) solution using a Varian EM360 magnet that was controlled with an Anasazi EFT60 spectroscopy system. Elemental analyses were carried out by Galbraith Laboratories.

Synthesis of Porphyrin Derivatives. The (nitro)(pyridyl)cobalt(III) tetraphenylporphyrin derivatives were all prepared by the stoichiometric reaction of $\text{Co}^{\text{III}}\text{TPP}$ (Aldrich or Midcentury Chemicals) with AgNO_2 (Acros Organics, 99%) in the presence of pyridine or its derivatives in refluxing acetonitrile (Sigma) under nitrogen atmosphere according to the method of Andrews.³ All materials, except for dichloromethane solvent used for extraction in these syntheses, were used as received. It was important to remove the amylene stabilizer from this solvent prior to its use by washing with sulfuric acid, sodium hydroxide, and water before drying with calcium chloride and distilling from phosphorus pentoxide under nitrogen.⁵ The parent compound, (nitro)(pyridyl)cobalt(III) tetraphenylporphyrin, was also prepared by air oxidation of $\text{Co}^{\text{II}}\text{TPP}(\text{NO})$ in toluene in the presence of excess pyridine.⁶ The compounds were purified with column chromatography on silica gel (Fisher 35–60 mesh, type 60A) eluting first with toluene followed by a 10% solution of methanol in toluene. The second eluting orange-red porphyrin fraction contained the desired products.

(Pyridyl)(nitro)cobalt(III) Tetraphenylporphyrin, (py)Co^{III}TPP(NO₂). The previous synthetic procedure of Andrews³ et al. was followed, except for purification using column chromatography. The synthetic reactions were carried out under nitrogen using standard Schlenk techniques, but the compound was then handled in the air. FTIR: ν_{NO_2} 1425 cm^{-1} , ν_{NO_2} 1309 cm^{-1} , and $\delta_{\text{O-N-O}}$ 814 cm^{-1} . UV-vis: λ_{max} 436 nm. This compound was also made by the original method of Tovrog et al.² by air oxidation of $\text{Co}^{\text{II}}\text{TPP}(\text{NO})$ in toluene with excess pyridine. Crystals of the pyridyl solvate $(\text{py})\text{Co}^{\text{III}}\text{TPP}(\text{NO}_2) \cdot 1/2(\text{pyridine})$ were grown by vapor diffusion of hexane into ~1 mM solutions of $\text{Co}^{\text{II}}\text{TPP}(\text{NO})$ originally dissolved under nitrogen atmosphere in ~1:1 toluene/methanol mixtures with pyridine at ~0.1 M. These solutions were allowed to react with air as crystallization took place over 2 weeks. A purple plate was selected for X-ray diffraction analysis.

(3,5-Lutidine)(nitro)cobalt(III) Tetraphenylporphyrin, (lut)Co^{III}TPP(NO₂). This compound was prepared from CoTPP with AgNO_2 oxidation in the presence of a stoichiometric quantity of 3,5-lutidine (Aldrich) in refluxing acetonitrile under nitrogen. Anal. Calcd for $\text{C}_{51}\text{H}_{39}\text{N}_6\text{O}_2\text{Co}$: C, 74.08; H, 4.75; N, 10.16. Found: C, 74.41; H, 4.48; N, 8.45. UV-vis: λ_{max} 436 nm. IR: ν_{NO_2} 1425 cm^{-1} , ν_{NO_2} 1307 cm^{-1} , and $\delta_{\text{O-N-O}}$ 815 cm^{-1} . This derivative was previously synthesized by oxidation of $\text{Co}^{\text{II}}\text{TPP}(\text{NO})$ in the presence of 3,5-lutidine and studied by X-ray diffraction methods.⁶

(4-*N,N*-Dimethylaminopyridyl)(nitro)cobalt(III) Tetraphenylporphyrin, (Me₂Npy)Co^{III}TPP(NO₂). This compound was prepared from CoTPP with AgNO_2 oxidation in the presence of a stoichiometric quantity of 4-*N,N*-dimethylaminopyridine (Aldrich) in refluxing acetonitrile under nitrogen. Anal. Calcd for $\text{C}_{51}\text{H}_{38}\text{N}_7\text{O}_2\text{Co}$: C, 72.93; H, 4.56; N, 11.67. Found: C, 71.90; H, 4.53; N, 12.58. UV-vis: λ_{max} = 438 nm. IR: ν_{NO_2} 1427 cm^{-1} , ν_{NO_2} 1310 cm^{-1} , and $\delta_{\text{O-N-O}}$ 813 cm^{-1} .

(3,5-Dichloropyridyl)(nitro)cobalt(III) Tetraphenylporphyrin, (Cl₂py)Co^{III}TPP(NO₂). This derivative was prepared only by the Andrews method using AgNO_2 oxidation of $\text{Co}^{\text{II}}\text{TPP}$ under N_2 atmosphere in the presence of at least 10-fold excess of 3,5-dichloropyridine, Cl_2py (Aldrich). The compound was purified by silica gel chromatography as described earlier. Crystallization of the porphyrin mixture in the presence of excess Cl_2py from CHCl_3 by evaporation or by vapor diffusion of hexane into toluene solutions resulted in a mixture of crystals. A red-purple parallelepiped crystal of $(\text{Cl}_2\text{py})\text{Co}^{\text{III}}\text{TPP}(\text{NO}_2) \cdot 1/2(\text{CHCl}_3)$ was selected for X-ray data collection. Anal. Calcd for $\text{C}_{49}\text{H}_{31}\text{N}_6\text{O}_2\text{Cl}_2\text{Co}$: C, 67.98; H, 3.609; N, 9.708. Found: C, 66.79; H, 4.45; N, 8.10. UV-vis: λ_{max} = 431 nm. IR: ν_{NO_2} 1424 cm^{-1} , ν_{NO_2} 1309 cm^{-1} , and $\delta_{\text{O-N-O}}$ 817 cm^{-1} .

Solution Phase (Nitro)(tetraphenylporphinato)cobalt(II), CoTPP(NO₂). Solution preparation of $\text{CoTPP}(\text{NO}_2)$ was carried out by reactions of $(\text{Cl}_2\text{py})\text{CoTPP}(\text{NO}_2)$ with lithium perchlorate in CH_2Cl_2 . This species was also observed in equilibrium with $(\text{Cl}_2\text{py})\text{CoTPP}(\text{NO}_2)$ and $(\text{py})\text{CoTPP}(\text{NO}_2)$ in CH_2Cl_2 solution at low concentrations. UV-vis: λ_{max} = 417 nm. It has also been previously reported by Andrews as part of a mixture in the solid state with assigned infrared bands ν_{sNO_2} of 1283 cm^{-1} and ν_{aNO_2} of 1453 cm^{-1} .

(3,5-Dichloropyridyl)(nitro)(tetra- $\alpha,\alpha',\alpha'',\alpha'''$ -(*o*-pivalamido-phenyl)porphinato)cobalt(III), (Cl₂py)Co^{III}TpivPP(NO₂). This picket-fence porphyrin derivative was prepared only by the Andrews method using AgNO_2 oxidation of $\text{Co}^{\text{II}}\text{TpivPP}$ under N_2 atmosphere in the presence of at least 10-fold excess of 3,5-dichloropyridine, Cl_2py (Aldrich). The compound was purified by silica gel chromatography.

Porphyrins Adsorbed on Silica Gel. (Nitro)cobaltTPP was adsorbed onto silica gel (Sigma Type G with CaSO_4 binder, 10–40 μm) by low-pressure evaporation of CH_2Cl_2 solutions of $(\text{Cl}_2\text{py})\text{CoTPP}(\text{NO}_2)$ alone and in the presence of LiClO_4 . Mass proportions of porphyrin to silica gel were roughly 1:50. $\text{CoTPP}(\text{NO})$ was adsorbed onto silica gel (1:10 proportions) by evaporation immediately after preparation in toluene solution by Schlenk techniques. The electronic spectrum before evaporation was taken under nitrogen atmosphere in the glovebox with an Ocean Optics PC1000 fiber optics spectrometer. The adsorbed $\text{CoTPP}(\text{NO})$ was redissolved with CH_2Cl_2 under nitrogen to produce an identical electronic spectrum with Soret position at 414 nm, consistent with the assignment of $\text{CoTPP}(\text{NO})$. Reflectance electronic spectra of the nitro derivatives were recorded using an Ocean Optics reflectance probe. Regardless of the method of preparation, the Soret peak appeared at 428 nm.

X-ray Crystallography. (py)Co^{III}TPP(NO₂)·1/2(pyridine). Data was collected with a Rigaku AFC7R diffractometer using graphite-monochromated $\text{Mo K}\alpha$ radiation ($\lambda = 0.71073 \text{ \AA}$) at a room temperature of $22 \pm 1 \text{ }^\circ\text{C}$. The structure was solved by direct methods and refined using full-matrix least-squares on F^2 (SHELXTL PLUS).

(Cl₂py)Co^{III}TPP(NO₂)·1/2(CHCl₃). Data was collected using a Rigaku AFC8/Mercury CCD using graphite-monochromated $\text{Mo K}\alpha$ radiation ($\lambda = 0.71073 \text{ \AA}$) at a room temperature of $22 \pm 1 \text{ }^\circ\text{C}$. The structure was solved by direct methods and refined using full-matrix least-squares on F^2 (SHELXTL PLUS).

Electrochemistry. Cyclic voltammetry was performed in a nitrogen-filled glovebox (Vacuum Atmospheres) using a EG&G VersaStat system and a three-electrode arrangement of a Cypress Systems platinum minielectrode, a nonaqueous ($\text{Ag}/\text{AgNO}_3\text{--CH}_3\text{CN}$) reference electrode (Bioanalytical Systems), and a platinum wire counter electrode. Solutions were prepared in CH_2Cl_2 purified as described above. UV-visible spectra were checked immediately prior to electrochemistry experiments to ensure that no decomposition had occurred. The supporting electrolyte, tetrabutylammonium hexafluorophosphate, TBAH (Aldrich), was recrystallized from ethyl acetate three times and dried at $110 \text{ }^\circ\text{C}$ in a vacuum oven for 5 days.⁵ Its concentration in the electrochemistry was 0.10 M. A scan rate of 20 mV/s over the range of 0.0 to +2.0 V vs $\text{Ag}/\text{AgNO}_3\text{--CH}_3\text{CN}$ was used for all measurements. Ferrocene was used as an internal standard. Solutions were initially prepared as 1 mM in porphyrin, tested for purity by UV-visible spectroscopy in the glovebox, and immediately examined by cyclic voltammetry. Generation of the pentacoordinate nitro complex in solution was carried out by saturating the test solution of $(\text{Cl}_2\text{py})\text{Co}^{\text{III}}\text{TPP}(\text{NO}_2)$.

(4) Munro, O. Q.; Scheidt, W. R. *Inorg. Chem.* **1998**, *37*, 2308–2316.

(5) Armarego, W. L. F.; Perrin, D. D. *Purification of Laboratory Chemicals*, 4th ed.; Butterworth–Heinemann: Oxford, 1996.

(6) Kaduk, J. A.; Scheidt, W. R. *Inorg. Chem.* **1974**, *13*, 1875–1880.

Table 1. Summary of Measured and Predicted Nitro Ligand Structural Features

	Hammett params	measd O–N–O bond angle, deg [av] (predicted) ^b	measd NO bond lengths, Å [av] (predicted)	measd Co–N _{nitro} bond lengths, Å (predicted)	measd Co–N _{py} bond lengths, Å (predicted)
(Cl ₂ py)CoTPP(NO ₂)	$\sigma_m = +0.64^a$	119.7(4) (120.66)	1.215(4) 1.220(4) (1.223)	1.912(3) (1.877)	1.952(3) (1.956)
(py)CoTPP(NO ₂)	$\sigma_p = 0$ $\sigma_m = 0$	118.9(9) 121.6(13) 122.5(8) 119.3(11) [120.6(21)] (120.39)	1.357(16) 1.245(12) 1.079(17) 1.197(15) [1.220(16)] (1.223)	1.920(4) (1.878)	2.032(4) (1.961)
(lut)CoTPP(NO ₂) ^c	$\sigma_m = -0.10$	115.4(6) (120.53)	1.155(5) (1.224)	1.948(4) (1.878)	2.036(4) (1.958)
(Me ₂ Npy)CoTPP(NO ₂)	$\sigma_p = -0.80^a$	NA (120.52)	NA (1.224)	NA (1.878)	NA (1.955)
CoTPP(NO ₂)		(124.41)	(1.220)	(1.832)	NA
(F ₃ py)CoTPP(NO ₂)	$\sigma = +2.60$	(122.09)	(1.221)	(1.844)	(2.414)
(ClO ₄)CoTPP(NO ₂)	NA	(121.10)	(1.222)	(1.862)	
(1-MeIm)CoTpvPP(NO ₂)		119.8(4) (120.09)	1.223(3) (1.224)	1.898(4) (1.875)	1.995(4) (1.955)
(1,2-Me ₂ Im)CoTpvPP(NO ₂)		120.4(4) (119.96)	1.227(3) (1.224)	1.917(4) (1.876)	2.091(4) (1.970)
(pip)CoTPP(NO ₂)		115.4(11) (120.92)	1.182(14) 1.207(14) (1.223)	1.897(11) (1.869)	2.044(10) (2.064)

^a Hammett values were calculated according to the equation $\sigma = \log(K_a/K_{a0})$ where K_a is for the identically substituted benzoic acid derivative. These pK_a 's were obtained through the result of ACD/pK_a DB v 4.0 that was accessed through the ACD/I-Lab Service. The pK_a of 3,5-dichlorobenzoic acid = 3.56, the pK_a of 4-*N,N*-dimethylaminobenzoic acid = 5.00, the pK_a of 3,6-dimethylbenzoic acid = 4.30, and the pK_a of pentafluorobenzoic acid = 1.60. These were all compared to the pK_a of benzoic acid of 4.202. ^b Predicted by semiempirical calculations of equilibrium geometries using the PM3 basis sets. ^c lut = 3,5-lutidine. The X-ray crystal structure of this derivative was reported by Kaduk and Scheidt.⁴

CoTPP(NO₂) with LiClO₄. No corrections to the current were made for increased ionic strength due to this addition.

Computational Modeling. Semiempirical calculations were carried out using PM3 basis sets with PC Spartan Plus (Wavefunction, Inc.). Equilibrium geometries and vibrational frequencies of the nitro ligands were determined for all of the hexacoordinate (py)CoTPP(NO₂) derivatives and for the pentacoordinate CoTPP(NO₂) derivative. No corrections were made to the calculated vibrational frequencies.

Equilibrium Measurements. Equilibrium of association of the respective pyridine ligands with the (nitro)cobalt tetraphenylporphyrins was studied by UV–visible spectrophotometry in CH₂Cl₂ solution by preparing a series of solutions with constant porphyrin concentration, but with varying concentration of the pyridine ligand. Data were analyzed for both the single equilibrium of association of the pyridine ligand and for the limiting molar absorptivities of the equilibrium species by use of the PC/DOS version of the SPECDEC program.⁷ Eight wavelengths ranging from 360 to 465 nm and six solution concentrations of the pyridine ligand were used for each experiment. Linear baseline corrections were applied to the spectral data.

Reaction Studies. The stoichiometric oxidation of triphenylphosphine, PPh₃, that results in formation of triphenylphosphine oxide and (nitrosyl)cobalt(II) tetraphenylporphyrin as described by Tovrog^{2a} was used initially to compare oxo-transfer reactivity of the derivatives. These experiments were carried out under nitrogen atmosphere to allow observation of the reduction reaction of the porphyrin complex without the complication of ensuing oxidation by air. Solutions of porphyrins with and without added pyridine derivative in solution were freshly prepared under nitrogen, and solid triphenylphosphine was added and dissolved immediately. Comparisons in oxo-transfer reactivity were also made by anaerobic addition of allyl bromide to solutions of porphyrins in dichloromethane solution.

Potential disproportionation reactions⁴ were also monitored under nitrogen atmosphere by UV–visible spectroscopy in solutions of porphyrins prepared from freshly made solid samples. Lithium perchlorate additions were made immediately prior to data collection under

nitrogen atmosphere. Further reactions with pyridine additions were also carried out under nitrogen atmosphere.

Catalytic oxidation reactions with alkenes were qualitatively studied by allowing solutions of (Cl₂py)CoTPP(NO₂) (~1 mM) in CH₂Cl₂ (~1 mL) to react at room temperature with excess (1 mL) cyclohexene (Acros), allyl bromide (Acros), and styrene (Acros, stabilized with 10–15 ppm *p-tert*-butylcatechol). Reactions were carried out in an oxygen-rich atmosphere in vials capped with toy latex balloons filled with dioxygen gas attached and were allowed to proceed either in the dark or under fluorescent laboratory lighting. Samples were prepared with and without addition of lithium perchlorate to the solutions. Catalysts adsorbed on silica gel were reacted with neat liquid alkenes with the same type of oxygen-filled balloon. The products of these reactions were determined by GC–MS using a Hewlett-Packard 6890 GC system with a 5793 ion selective detector.

Results Section

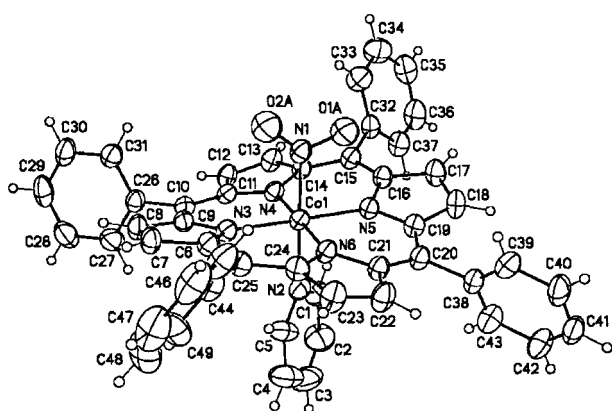
Computational Modeling. Results for the calculations of the equilibrium geometries by semiempirical methods using PM3 basis are tabulated in Table 1. In this table are listed measured and calculated nitro ligand NO bond lengths, Co–N_{nitro} and Co–N_{py} bond lengths, and nitro ONO bond angles for pyridine derivatives prepared in this work. Also listed are calculated results for the proposed pentacoordinate nitro species and the hypothetical pentafluoropyridyl derivative. While both the calculated and measured nitro ligand parameters are quite consistent for the pyridyl derivatives actually prepared in this work, complete removal of the pyridine ligand in the calculations gives a significantly larger ONO bond angle of 124° compared to the 120° angles predicted for the pyridyl derivatives. The semiempirical model of the hypothetical pentafluoropyridyl and perchlorate derivatives gave intermediate values of 122° and 121° for the respective ONO bond angles and a large increase in the Co–N_{pyr} bond length from roughly 2 to 2.4 Å for the pentafluoropyridyl derivative.

(7) Atkins, C. E.; Park, S. E.; Blaszcak, J. A.; McMillin, D. R. *Inorg. Chem.* **1984**, *23*, 569–572.

Table 2. Crystallographic Data for (py)CoTPP(NO₂)·0.5(py) and (Cl₂py)CoTPP(NO₂)·0.5(CHCl₃)

chem formula	C ₄₉ H ₃₃ N ₆ O ₂ Co· 0.5(C ₅ H ₅ N)	C ₄₉ H ₃₁ N ₆ O ₂ Cl ₂ Co· 0.5(CHCl ₃)
fw	836.29	925.35
space group	<i>P</i> 2 ₁ / <i>n</i> (No. 14)	<i>P</i> 2 ₁ / <i>n</i> (No. 14)
<i>a</i> (Å)	13.231(3)	13.3698(9)
<i>b</i> (Å)	23.566(3)	23.216(3)
<i>c</i> (Å)	14.537(2)	15.1300(3)
β (deg)	101.02(1)	105.613(3)
<i>V</i> (Å ³)	4449(1)	4523.1(5)
<i>Z</i>	4	4
<i>T</i> (°C)	22 ± 1	22 ± 1
<i>D</i> _{calcd} (g cm ⁻³)	1.25	1.36
λ (Å)	0.71073	0.71073
μ (cm ⁻¹)	4.3	6.3
R1 (<i>F</i> _o ²) ^a	0.065	0.059
wR2 (<i>F</i> _o ²) ^b	0.213	0.193

^a $R1 = \sum ||F_o| - |F_c|| / \sum |F_o|$ for $I > 2\sigma(I)$. ^b $wR2 = \{\sum [w(F_o^2 - F_c^2)]^2 / \sum [w(F_o^2)]^2\}^{1/2}$ for all data.

**Figure 1.** ORTEP plot of (py)CoTPP(NO₂) at the 30% probability level.

Crystal Structures. (py)CoTPP(NO₂)·1/2(py). The parent pyridine derivative crystallized in the monoclinic *P*2₁/*n* space group with four porphyrin molecules per unit cell. The unit cell dimensions were *a* = 13.231(3) Å, *b* = 23.566(3) Å, and *c* = 14.537(2) Å; β = 101.02(1)°. The crystallographic data is summarized in Table 2. Disorder in the nitro ligand was modeled by four equivalent oxygen atoms at half-occupancy. The molecular structure of the porphyrin is illustrated at the 30% probability level in the ORTEP diagram in Figure 1. Bond lengths and angles are listed in Table 3A. Nitro ligand bond lengths and angles are compared with those determined by semiempirical modeling in Table 1.

(Cl₂py)CoTPP(NO₂). The pyridyl derivative of CoTPP(NO₂) prepared with the most weakly coordinating pyridine ligand, (Cl₂py)CoTPP(NO₂), also crystallized in the monoclinic *P*2₁/*n* space group with four porphyrin molecules per unit cell. The unit cell dimensions were *a* = 13.3698(9) Å, *b* = 23.216(3) Å, and *c* = 15.130(3) Å; β = 105.613(3)°. The crystallographic data is summarized in Table 2. The molecular structure of the porphyrin is illustrated in the ORTEP diagram at the 30% probability level in Figure 2. Bond lengths and angles are in Table 3B. Nitro ligand bond lengths and angles are compared with those determined by semiempirical modeling in Table 1.

Spectroscopy. The infrared spectra of (py)CoTPP(NO₂) and of its reduced analogue CoTPP(NO) have been used to monitor the formation and to assess the nature of these compounds in reaction studies.^{2a} In the series of pyridine derivatives, only slight differences in the positions of the characteristic bands of the nitro ligand ν_{asNO_2} , ν_{sNO_2} and $\delta_{\text{O-N-O}}$ were observed. These

Table 3. Bond Distances and Angles of the Cobalt Coordination Site for (py)CoTPP(NO₂)·1/2(py) and (Cl₂py)CoTPP(NO₂)·1/2(CHCl₃)

(A) (py)CoTPP(NO ₂)·1/2(py)			
Distances (Å)			
Co(1)–N(1)	1.920(4)	Co(1)–N(5)	1.959(3)
Co(1)–N(4)	1.964(3)	Co(1)–N(6)	1.974(4)
Co(1)–N(3)	1.977(4)	Co(1)–N(2)	2.032(4)
O(1A)–N(1)	1.357(16)	O(2A)–N(1)	1.079(17)
O(1B)–N(1)	1.245(12)	O(2B)–N(1)	1.197(15)
O(1C)–N(1)	1.254(13)	O(2C)–N(1)	1.22(2)
Angles (deg)			
N(1)–Co(1)–N(5)	88.50(16)	N(1)–Co(1)–N(4)	90.24(16)
N(5)–Co(1)–N(4)	89.59(14)	N(1)–Co(1)–N(6)	90.76(16)
N(5)–Co(1)–N(6)	90.43(15)	N(4)–Co(1)–N(6)	179.00(16)
N(1)–Co(1)–N(3)	90.79(16)	N(5)–Co(1)–N(3)	179.20(15)
N(4)–Co(1)–N(3)	90.05(15)	N(6)–Co(1)–N(3)	89.95(15)
N(1)–Co(1)–N(2)	178.63(17)	N(5)–Co(1)–N(2)	90.14(15)
N(4)–Co(1)–N(2)	89.91(16)	N(6)–Co(1)–N(2)	89.09(16)
N(3)–Co(1)–N(2)	90.57(16)	O(2B)–N(1)–O(1B)	118.9(9)
O(2C)–N(1)–O(1C)	121.6(13)	O(2A)–N(1)–O(1A)	118.7(12)
O(2A)–N(1)–Co(1)	125.0(10)	O(2B)–N(1)–Co(1)	122.5(8)
O(2C)–N(1)–Co(1)	119.3(11)	O(1B)–N(1)–Co(1)	116.7(6)
O(1C)–N(1)–Co(1)	118.2(6)	O(1A)–N(1)–Co(1)	116.0(7)

(B) (Cl ₂ py)CoTPP(NO ₂)·1/2(CHCl ₃)			
Distances (Å)			
Co(1)–N(1)	1.912(3)	Co(1)–N(5)	1.952(3)
Co(1)–N(6)	1.952(3)	Co(1)–N(4)	1.955(3)
Co(1)–N(3)	1.959(3)	Co(1)–N(2)	2.044(3)
O(1)–N(1)	1.215(4)	O(2)–N(1)	1.220(4)
Angles (deg)			
N(1)–Co(1)–N(5)	90.83(13)	N(1)–Co(1)–N(6)	90.86(13)
N(5)–Co(1)–N(6)	89.77(12)	N(1)–Co(1)–N(4)	89.57(13)
N(5)–Co(1)–N(4)	90.77(12)	N(6)–Co(1)–N(4)	179.30(13)
N(1)–Co(1)–N(3)	91.87(14)	N(5)–Co(1)–N(3)	177.10(13)
N(6)–Co(1)–N(3)	89.13(12)	N(4)–Co(1)–N(3)	90.30(12)
N(1)–Co(1)–N(2)	179.31(14)	N(5)–Co(1)–N(2)	89.84(13)
N(6)–Co(1)–N(2)	88.97(12)	N(4)–Co(1)–N(2)	90.59(13)
N(3)–Co(1)–N(2)	87.45(13)	O(1)–N(1)–O(2)	119.7(4)
O(1)–N(1)–Co(1)	119.6(3)	O(2)–N(1)–Co(1)	120.7(3)
C(5)–N(2)–C(1)	118.7(4)	C(5)–N(2)–Co(1)	120.6(3)
C(1)–N(2)–Co(1)	120.4(3)	C(6)–N(3)–C(9)	105.8(3)
C(6)–N(3)–Co(1)	126.6(2)	C(9)–N(3)–Co(1)	126.9(2)
C(11)–N(4)–C(14)	106.4(3)	C(11)–N(4)–Co(1)	126.6(3)
C(14)–N(4)–Co(1)	126.6(2)	C(16)–N(5)–C(19)	105.7(3)
C(16)–N(5)–Co(1)	127.2(2)	C(19)–N(5)–Co(1)	126.9(2)
C(24)–N(6)–C(21)	105.8(3)	C(24)–N(6)–Co(1)	127.1(2)
C(21)–N(6)–Co(1)	127.0(2)	N(2)–C(1)–C(2)	121.1(4)

values are listed in Table S1 in the Supporting Information. The slight variation of these positions shows trends with the Hammett parameters determined for these pyridine derivatives.

The electronic spectrum of (nitro)(pyridyl)cobalt(III) porphyrin has not been reported previously. The position of the Soret peaks of the pyridyl derivatives was also found to vary slightly with the basicity of the pyridine ligand according to Hammett parameters as reported in Table S1. These values ranged from 432 nm for the least basic pyridine derivative, Cl₂py, to 438 nm for the most basic derivative, Me₂Npy. The similarity of the position of the Soret peaks for CoTPP (411 nm), CoTPP(NO) (414 nm),⁸ and the proposed pentacoordinate species, CoTPP(NO₂) (417 nm), led to confusion about the identity of this latter species. Recent thin-film experiments by Kurtikyan et al. have provided evidence for the formation of CoTPP(NO₂) in the solid state by two methods: (1) direct

(8) Richter-Addo, G. B.; Hodge, S. J.; Yi, G. -B.; Khan, M. A.; Ma, T.; Van Caemelbecke, E.; Guo, N.; Kadish, K. M. *Inorg. Chem.* **1996**, *35*, 6530–6538.

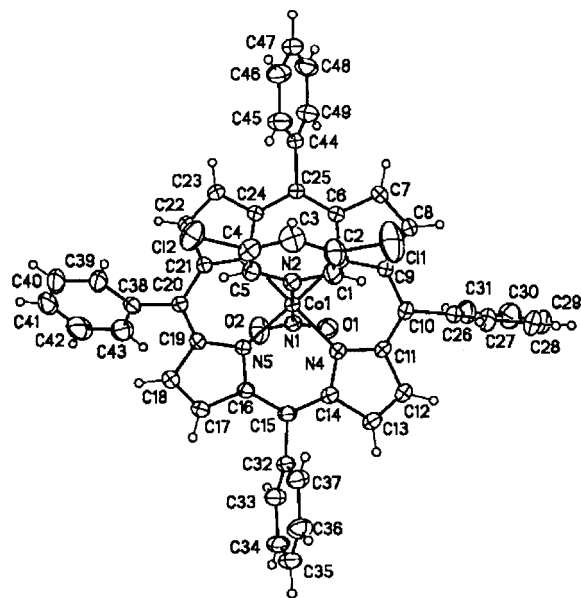


Figure 2. ORTEP plot of $(\text{Cl}_2\text{py})\text{CoTPP}(\text{NO}_2)$ at the 30% probability level.

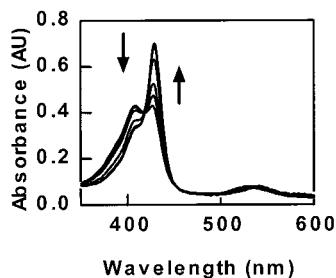


Figure 3. Electronic spectra of solutions of partially dissociated (pyridyl)(nitro)cobalt(III) porphyrin complexes in CH_2Cl_2 and during titration of excess pyridine ligand, used in determination of equilibrium constants for pyridine association: $(\text{Cl}_2\text{py})\text{CoTPP}(\text{NO}_2)$ (8.78×10^{-6} M with Cl_2py concentrations ranging from 8.78×10^{-6} M to 2.5×10^{-5} M).

reaction of NO_2 gas with sublimed CoTPP^9 and reaction of O_2 gas with $\text{CoTPP}(\text{NO})^{10}$ prepared in the solid state by reaction of NO gas with CoTPP . The reported electronic spectrum that has its Soret position at ~ 422 nm is similar to our observations of the $\text{CoTPP}(\text{NO}_2)$ in CH_2Cl_2 solution.

Coordination Equilibria. At low concentrations ($\sim 10^{-6}$ M in CH_2Cl_2), both $(\text{Cl}_2\text{py})\text{CoTPP}(\text{NO}_2)$ and $(\text{py})\text{CoTPP}(\text{NO}_2)$ derivatives show two Soret peaks, even after careful purification of the porphyrins by column chromatography. Initially the second, higher energy band in the 414–417 nm region was assigned as contaminant CoTPP (411 nm) or $\text{CoTPP}(\text{NO})$ (414 nm) arising from incomplete reaction or decomposition of the nitro derivative. Figure 3 shows the electronic spectrum of this equilibrium mixture generated by dissolving $(\text{Cl}_2\text{py})\text{CoTPP}(\text{NO}_2)$ in CH_2Cl_2 under nitrogen atmosphere, and the resulting spectra as Cl_2py is titrated into the solution, the porphyrin concentration being held constant. The isosbestic behavior of these spectra implies that a clean conversion from a proposed pentacoordinate $\text{CoTPP}(\text{NO}_2)$ species to $(\text{Cl}_2\text{py})\text{CoTPP}(\text{NO}_2)$ is observed during these additions. The value of the equilibrium constant at 25°C for association of the Cl_2py ligand was 6.94×10^6 with a value of $\chi^2 = 7.2 \times 10^{-4}$ reported by the

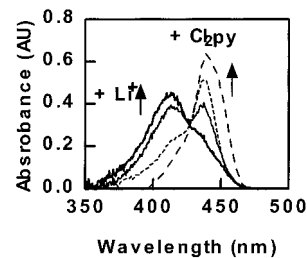


Figure 4. Electronic spectra of partially dissociated $(\text{Cl}_2\text{py})\text{CoTPP}(\text{NO}_2)$ (\cdots) in CH_2Cl_2 under nitrogen and the same solution after addition of solid LiClO_4 (saturated solution) (—). Spectra were recorded at times of 1 and 3 min. The solution was then saturated with Cl_2py and immediately converted to the spectrum of fully associated $(\text{Cl}_2\text{py})\text{CoTPP}(\text{NO}_2)$ (---).

SPECDEC program. The value for the association of the pyridine ligand, found by the same method, was based upon the spectra shown in Figure S1 in the Supporting Information. The value of the equilibrium constant for the pyridine ligand was found to be 1.08×10^8 with $\chi^2 = 1.29 \times 10^{-4}$. None of the other pyridyl derivatives show the higher energy band attributed to $\text{CoTPP}(\text{NO}_2)$ even at low concentration, so no attempts were made to measure their stability constants. This behavior is consistent with their greater basicities as reflected in their Hammett values.

The reactions with the lithium ion with $(\text{Cl}_2\text{py})\text{CoTPP}(\text{NO}_2)$ in CH_2Cl_2 was followed by UV–visible spectroscopy as shown in Figure 4. As noted previously, at solution concentrations in the 1×10^{-5} M range, the Cl_2py ligand is largely dissociated. The figure shows the peaks at 431 nm assigned to the associated $(\text{Cl}_2\text{py})\text{CoTPP}(\text{NO}_2)$ and the peak at 417 nm assigned to $\text{CoTPP}(\text{NO}_2)$. Upon addition of lithium perchlorate, the Cl_2py is lost from the complex within 10 min as shown in the figure. Addition of a large excess of Cl_2py to the same solution results in complete re-formation of the complex instantly as shown by the single peak at 432 nm represented by the dashed line.

Electrochemistry. Cyclic voltammetry of the series of derivatives is more sensitive to the variation of the pyridine ligand coordination equilibrium than the static structural results given by crystal structures or spectroscopy. The cyclic voltammogram for the most stable derivative, $(\text{Me}_2\text{Npy})\text{CoTPP}(\text{NO}_2)$, is shown in Figure S2 in the Supporting Information and provides three clear quasi-reversible couples. The half-wave potentials of all the derivatives reported in volts vs the $\text{Ag}/\text{AgNO}_3(\text{CH}_3\text{CN})$ reference electrode are listed in Table 4. Upon addition of excess LiClO_4 to the solution of $(\text{Cl}_2\text{py})\text{CoTPP}(\text{NO}_2)$, the pattern of three quasi-reversible processes quickly changes to a single irreversible oxidation within the range 0.4–2.0 V as shown in Figure S3 in the Supporting Information.

Reactions. In the reaction of $(\text{Cl}_2\text{py})\text{CoTPP}(\text{NO}_2)$ with Ph_3P (50 mM) with added LiClO_4 , the electronic spectra in Figure S4 (Supporting Information) show rapid conversion to three products with new Soret peak positions at 414, 447, and 467 nm. The peak position at 414 nm is again ambiguous, but may be attributed to the $\text{CoTPP}(\text{NO})$ species since its formation may be followed by IR spectroscopy. The other peaks at 447 and 467 nm appear on the same rapid time scale. Further addition of Ph_3P increases the intensity of the peak at 467 nm while decreasing the intensity of the peak at 447 nm. These two peaks are proposed to be a (triphenylphosphino)(nitro)cobalt(III) complex, $(\text{Ph}_3\text{P})\text{CoTPP}(\text{NO}_2)$, and the bis(triphenylphosphino)cobalt(III) complex, respectively.

Electronic spectra collected over the course of the reaction of triphenylphosphine (2 mM) with $(\text{Me}_2\text{Npy})\text{CoTPP}(\text{NO}_2)$ (1

(9) Kurtikyan, T. S.; Stepanyan, T. G.; Gasparyan, A. V. *Russ. J. Coord. Chem.* **1997**, *23*, 563–567.

(10) Kurtikyan, T. S. *Russ. J. Coord. Chem.* **1999**, *25*, 28–30.

Table 4. Electrochemical and Stability Constant Effects of the Distal Pyridine Ligand

	Hammett params	$E_{1/2}^a$ [$E_{1/2}$] ^b (ΔE_p) ^c	$E'_{1/2}$ [$E'_{1/2}$] (ΔE_p)	$E''_{1/2}$ [$E''_{1/2}$] (ΔE_p)	K
(Cl ₂ py)CoTPP(NO ₂)	$\sigma_m = +0.64$	0.71 [0.95] (120)	1.07 [1.31] (190)	1.28 [1.52] (160)	6.94×10^6
(py)CoTPP(NO ₂) ^d	$\sigma_p = 0$	0.69 [0.93] (180)	0.90 [1.14] (160)	1.21 [1.45] (220)	1.08×10^8
(3,5-lut)CoTPP(NO ₂)	$\sigma_m = -0.10$	0.67 [0.91] (140)	1.01 [1.25] (220)	1.27 [1.51] (220)	<i>h</i>
(Me ₂ Npy)CoTPP(NO ₂)	$\sigma_p = -0.80$	0.63 [0.87] (100)	0.92 [1.16] (160)	1.11 [1.35] (100)	<i>h</i>
“CoTPP(NO ₂)” ^d	NA	1.24 ^e [1.48]			
CoTPP(NO)	NA	$E_{1/2}(+/0)^{f,g}$ 1.00 ^f 1.01 ^g	$E_{1/2}(+/2+)^{f,g}$ 1.37 ^f 1.25 ^g		

^a All values determined in 0.10 M TBAH, reported in volts vs Ag/AgNO₃ in CH₃CN. Ferrocene as an internal standard gave an $E_{1/2}$ of 0.240 V with this electrode. ΔE_p for this reference peak was found to be 160 mV. No corrections were made for junction potentials. All measurements made on compounds without added pyridine ligand, except for Cl₂py, with 0.1 M ligand added. ^b Values corrected to SCE. ^c ΔE_p values given in mV. ^d Obtained by reacting the solution of (Cl₂py)CoTPP(NO₂) with saturated LiClO₄. ^e Irreversible oxidation peak potential. ^f Values and assignments reported by Kini et al.¹⁶ ^g Values and assignments reported by Richter-Addo et al.⁸ ^h Coordination equilibria were not observable.

$\times 10^{-5}$ M) with added Me₂Npy (50 mM) also show formation of peaks assignable to (Ph₃P)CoTPP(NO₂) and CoTPP(NO). Direct comparison of oxo-transfer reactivity with triphenylphosphine is complicated by the substitution chemistry with triphenylphosphine.

The electronic spectra showing the reaction of (Cl₂py)CoTPP(NO₂) with allyl bromide (0.5 M) are shown in Figure S5 in the Supporting Information. In this reaction in CH₂Cl₂ under N₂, no additional lithium perchlorate was added. The rapid partial formation of the peak at 414 nm is consistent with the formation of CoTPP(NO) from free CoTPP(NO₂) with a slower reaction taking place as Cl₂py dissociates from the complex leaving the reactive CoTPP(NO₂) available for rapid oxidation of the allyl bromide. A similar procedure was used to compare the oxo-transfer reactivity of the fully complexed (Me₂Npy)-CoTPP(NO₂) with allyl bromide. Under anaerobic conditions and with excess Me₂Npy (0.010 M) in solution, there is *no detectable reaction* of (Me₂Npy)CoTPP(NO₂) with allyl bromide in dichloromethane solution monitored over the course of 3 days.

Reactions under oxygen atmosphere have qualitatively shown a wide range of catalytic oxidation reactions, depending upon the conditions of the experiment as summarized in Table 5. Room temperature catalytic oxidation of a large excess of cyclohexene (1 mL added to 1 mL of 1 mM [(Cl₂py)CoTPP(NO₂)] in 1 mL of CH₂Cl₂) exposed to fluorescent room lighting produced 2-cyclohexen-1-ol, 3-cyclohexen-1-ol, 1,2-cyclohexanediol, cyclohexene oxide, 2-cyclohexen-1-one, 1,2-cyclohexanedione, and bi-2-cyclohexen-1-yl after 1 day with roughly half of the cyclohexene remaining, corresponding to a catalytic turnover of ~ 6000 (cyclohexene/cobalt) and a TOF of ~ 5 cyclohexene·cobalt⁻¹·min⁻¹. Roughly the same results were observed with this reaction carried out in the dark. Oxidation of styrene with light exposure under the same reaction conditions gives benzaldehyde, styrene oxide, α -methylstyrene, benzene acetaldehyde, phenylethyl alcohol, 1-phenyl-1,2-ethanediol, and benzoylformic acid. A similar distribution of products was observed for the reaction carried out in the dark. Oxidation reactions of allyl bromide in the light under similar conditions produced a wide range of products including 1,3-dibromopropanol, 2,3-dimethyl-2,3-butanediol, the ethyl ester of 3-bromo-

2-oxopropionic acid, and 1,2-dibromocyclohexane. A similar range of products was obtained for the reaction carried out in the dark. The products are illustrated in Table 5.

Reactions that were carried out with silica gel adsorbed CoTPP(NO₂) and neat cyclohexene gave much simpler product distributions with roughly the same rate of loss of reactant. Regardless of the method of synthesis of the catalyst, the products obtained were cyclohexen-2-ol, cyclohexen-2-one, cyclohexene oxide, and bi-2-cyclohexen-1-yl, with appearance of the last species occurring only after several days of reaction. The proportions of products in the first 2 days showed that the sum of the cyclohexene oxide and cyclohexen-2-one was roughly equal to the total amount of the alcohol produced.

Catalytic oxidation products obtained with silica gel adsorbed CoTPP(NO) from neat cyclohexene and O₂ were the same as those obtained from the adsorbed (nitro)cobalt porphyrin catalysts.

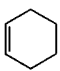
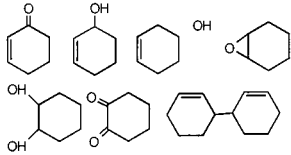
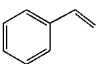
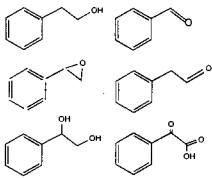
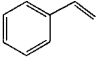
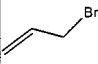
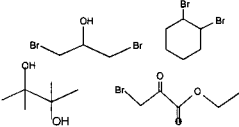
The (Cl₂py)CoTpivPP(NO₂)-catalyzed oxygenation reactions with cyclohexene and allyl bromide provided product distributions similar to those obtained with the unhindered porphyrin catalysts. However, for the reaction with styrene, *virtually no reactivity was observed for the hindered (dichloropyridyl)-(nitro)cobalt(III) picket-fence porphyrin*.

Discussion Section

Table 1 summarizes the predicted structural effects of the distal pyridine ligands on the nitro ligand. The variation in the basicity of the distal ligand results in only small changes in the N–O bond lengths and O–N–O bond angles. Exceptions appear where the very weak Lewis base pentafluoropyridine or the weakly coordinating perchlorate ion are used as the distal ligand. Even so, a correlation of these small changes with Hammett parameters for the pyridine ligands is evident from examination of the predictions.

The two crystal structures of this study are the fifth and sixth structures of (nitro)cobalt(III) porphyrins to be reported. The cobalt coordination site and nitro ligand bond angles and distances of two early structures of piperidine and 3,5-lutidine derivatives of CoTPP(NO₂) and of 1-methylimidazole and 1,2-dimethylimidazole derivatives of CoTpivPP(NO₂) are listed

Table 5. Products of Alkene Oxidation by O₂ as Catalyzed by (Cl₂py)CoTPP(NO₂) and (Cl₂py)CoTpivPP(NO₂)^a

Catalyst, solvent	Alkene	Conditions	Products
(Cl ₂ py)CoTPP(NO ₂), (Cl ₂ py)CoTpivPP(NO ₂), CH ₂ Cl ₂		Room temperature = 25±2°C, room light and dark	
(Cl ₂ py)CoTPP(NO ₂), CH ₂ Cl ₂		Room temperature = 25±2°C, room light	
(Cl ₂ py)CoTpivPP(NO ₂), CH ₂ Cl ₂		Room temperature = 25±2°C, room light	No Reaction
(Cl ₂ py)CoTPP(NO ₂), (Cl ₂ py)CoTpivPP(NO ₂), CH ₂ Cl ₂		Room temperature = 25±2°C, room light or dark	

^a Determined by GC–MS analysis of solutions after 24 h at room temperature.

along with those obtained here in Table 1. The nitro bond angles and distances for the lutidine and piperidine structures are noticeably smaller than those of any of the other derivatives. But problems associated with the ligand disorder, different temperatures of data collection, and low-resolution data collection make detailed comparison of nitro bond angles and lengths unreliable.

There are also minor trends in the observed spectroscopic measurements that correlate with predictions from semiempirical calculations as a function of ligands' basicities. Nitro ligand asymmetrical vibrational frequencies, ν_a , vary only slightly over the range of 1424–1427 cm⁻¹ according to the order of Hammett parameters. The calculated vibrational frequencies, while a poor match for the observed frequencies due to the approximations of the PM3 semiempirical model, are consistent with these small changes, ranging from 1812.58 to 1810.43 cm⁻¹. Andrews has reported the IR spectrum of the pentacoordinate species in a mixture with the acetonitrile complex. The asymmetrical stretching frequency, ν_a , of NO₂ was reported to be 1453 cm⁻¹ compared to the 1424–1427 cm⁻¹ observed for the hexacoordinate species in this work. The calculated value for the pentacoordinate complex was determined to be 1856 cm⁻¹ by the semiempirical model consistent in the observed increase in vibrational energy. Both calculated and observed symmetrical stretching frequencies show a decrease in vibrational energies with the loss of the pyridine ligand. The observed values for the pyridine complexes range from 1307 to 1310 cm⁻¹, but without the pyridine ligand, the value is 1283 cm⁻¹. The semiempirical model predicts a range of 1701.04 to 1702.65 cm⁻¹ for the pyridine complexes and 1673.79 cm⁻¹ for the respective symmetric vibrational frequencies. Vibrational frequency values for the hypothetical pentafluoropyridyl and perchlorato derivatives were also determined and are between

those of the pentacoordinate and the other hexacoordinate pyridyl derivative values as shown in the table. For electronic spectra, only the measured Soret peak positions were compared. These show variation from 432 nm for the weakest base (Cl₂py) to 438 nm for the strongest base (Me₂Npy). The loss of the sixth coordination site results in a shift of the Soret peak to 417 nm. It is noteworthy that, when CoTPP(NO₂) is deposited onto silica gel surfaces by a variety of methods, the consistently observed Soret position of 428 nm is between the values of the weakest pyridine base (432 nm) and the pentacoordinate species in solution (417 nm). A weak bonding interaction with the silica gel may give rise to this effect. Soret peak positions of 422 nm for the pentacoordinate nitro complex observed in its preparation by Kurtikyan are also between the Soret positions observed for the Cl₂py complex and the solution phase CoTPP(NO₂) species.

The pentacoordinate nitro complex demonstrates much greater secondary oxo-transfer reactivity than has been reported earlier. The existence of this species has been proposed earlier by Andrews and in the solid state by Kurtikyan, but its reactivity has not been recognized. In the presence of lithium perchlorate in large excess, it is conceivable that the perchlorate ion is weakly coordinated with the metal center as we observed in our study of the (nitro)iron(III) picket-fence porphyrin analogue.¹¹ Oxidation reactions using activation by lithium perchlorate as a cocatalyst were originally proposed to take place by an interaction with nitrite ligand through an NO₂ oxygen atom.^{2c} But the spectral changes represented in Figure 4 more strongly support pyridine removal in the presence of Li⁺ and addition of the pyridine ligand when it is added in excess. "Quenching" of oxo-transfer reactions by addition of excess

(11) Frangione, M.; Fangione, M.; Port, J.; Baldiwala, M.; Judd, A.; Galley, J.; DaVega, M.; Linna, K.; Caron, L.; Anderson, E.; Goodwin, J. *Inorg. Chem.* **1997**, *36*, 1904–1911.

pyridine has been discussed earlier for the pyridine complexes.⁶ We now interpret this effect as a result of promoting the formation of the unreactive hexacoordinate (py)CoTPP(NO₂) species and not as a result of formation of (py)₂CoTPP. For the reactions with triphenylphosphine, it is apparent that, with a reducing agent this strong, there is little difference in the reactivity of the hexacoordinated nitro complexes, and that ligand substitution by the triphenylphosphine ligand is a faster process than oxo transfer. Even in the presence of excess (Me₂-Npy) ligand, both ligand substitution and the eventual formation of the CoTPP(NO) product were observed.

The differences in reactivity of the pentacoordinate and hexacoordinate species are most evident in the reactions with alkenes. The Me₂Npy complex has been found not to react with any of the alkenes investigated in this project, even without additional Me₂Npy in CH₂Cl₂ solution. The equilibrium loss of the pyridine ligand indicated by the coordination equilibrium experiments can be promoted by the addition of the lithium ion which competes for the pyridine ligand. In using more strongly coordinating pyridine and higher concentrations of complexes, the reactions were not observed until the pentacoordinate species was generated by adding lithium perchlorate.

Since pyridine derivatives of (nitro)cobalt(III) porphyrin have been commonly prepared by O₂ oxidation of (nitrosyl)cobalt(II) porphyrins in the presence of the nitrogenous base, the intermediacy of the (nitrosyl)cobalt(II) species in the catalysis is suggested. Our observation that the same catalytic oxidation reactions occur for cyclohexene with oxygen with the silica-adsorbed CoTPP(NO) species strongly supports this species as an intermediate and indeed that the preparation of these solid phase catalysts could be greatly simplified with reactions of NO gas with solid adsorbed Co(II) porphyrins. Further mechanistic interpretation of this result follows later in this section.

In removal of the pyridine ligand by addition of Li⁺, the electrochemical behavior changes dramatically. Previous reports of the electrochemistry of CoTPP(NO) complexes suggests that the metal-centered oxidation for both series occurs at the extreme positive potential observed. The pyridine ligand dependence of all of the reversible couples listed in Table 5 is emphasized by the trend in all the half-wave potentials and the complete change in the electrochemical behavior upon the removal of the ligand. The identity of the irreversible oxidation wave is unknown at this time, but according to the trends expected with the basicity of the ligands, the potentials of all of the couples will be shifted to positive extremes. Assuming that this is the case, then the observed irreversible process for CoTPP(NO₂) has been shifted by nearly +0.5 V by the loss of the Cl₂py ligand that associates with an equilibrium constant of 6.94×10^6 .

The extreme shift in oxidation potential confers a much greater reactivity toward secondary oxo transfer as observed in the oxidation of alkenes that were previously reported to require "activation" by thallium or palladium cocatalysts, or simply nitro exchange to the palladium cocatalyst. The formation of alcohols by a C-H insertion and the coupled bi-2-cyclohexen-1-yl product suggests formation of O radicals as part of the catalytic oxidation mechanism.

The proposed mechanism involving the two distinct oxo-transfer steps is depicted in Figure 5. The radical mechanism could be promoted by interaction of excess dioxygen with the peroxynitro intermediate to form ozone. In Castro's study of ClFeTPP(NO₂), the formation of ozone from O₂ was confirmed as a route to the ensuing radical oxidation. Our semiempirical models included calculation of the heats of formation for the pentacoordinate peroxynitro derivative, CoTPP(NO, O₂), the

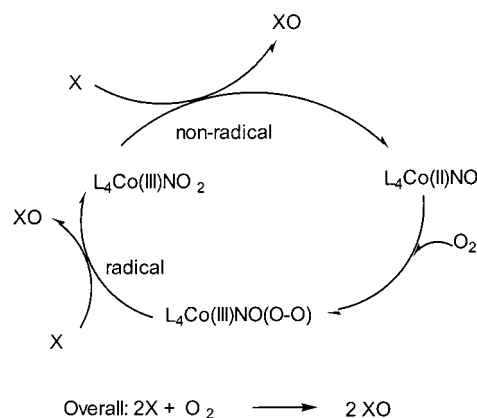


Figure 5. Proposed catalytic cycle for the oxidation of alkenes involving both bimolecular nonradical and radical oxo-transfer steps, through the formation of a peroxynitro intermediate that arises from the interaction of dioxygen with the reduced CoTPP(NO) form.

pentacoordinate nitro derivative, CoTPP(NO₂), dioxygen, and ozone. These results show a 114 kcal/mol thermodynamic advantage in the formation of the products CoTPP(NO₂) and ozone from dioxygen and the peroxynitro derivative. Related to this is Kurtikyan's observation¹¹ of the conversion of amorphous solid state CoTPP(NO) to CoTPP(NO₂) by reaction with gas phase O₂. Although those authors did not describe a mechanism for the reaction of the immobilized complex with dioxygen, the formation of a peroxynitro intermediate and its decomposition by further reaction with O₂ to form ozone and the product nitro complex is a rather simple explanation.

The dramatic difference in reactivity between styrene and the other alkenes with oxygen in the presence of (Cl₂py)CoTpvPP(NO₂) suggests that bimolecular oxo transfer is involved in the initial oxo-transfer step, since this is limited by the steric interactions of the picket-fence structure and the styrene molecule. The nitro ligand preferentially coordinates in the sterically hindered "pocket" and is only available for bimolecular oxo transfer with small molecules. A bimolecular oxo transfer has been invoked in nonradical mechanisms of epoxidation.

Therefore, two distinct oxo donors are envisioned in the catalytic cycle, consistent with the mechanism proposed by Basolo for the reaction of O₂ with cobalt nitrosyls to form nitro complexes. This mechanism includes the formation of the intermediate peroxynitro species which, in the absence of reducing agents, reacts with other nitrosyl complexes in a comproportionation reaction to form two molecules of the nitro complex.¹² If the initial oxo-transfer reaction from the nitro derivative occurs by a bimolecular mechanism, as suggested by the lack of reactivity between styrene and CoTpvPP(NO₂), then the further progress of the reaction by a radical pathway, not having the same steric constraints, would be ascribable to the proposed peroxynitro intermediate.

The decomposition of peroxynitrite by methemoglobin is currently of interest and related to the generation of oxygen radicals and catalytic regeneration of the nitro species in this study. Several groups of authors¹³⁻¹⁵ have debated the decomposition mechanism based upon UV-visible and EPR data and

- (12) Clarkson, S. G.; Basolo, F. *Inorg. Chem.* **1973**, *12*, 1528-1534.
- (13) Kahn, A. U.; Koviacic, D.; Kolbanovsky, A.; Desai, J.; Frenkel, K.; Geacintov, N. E. *Proc. Natl. Acad. Sci. U.S.A.* **2000**, *97*, 2984-2989.
- (14) Merenyi, G.; Link, J.; Czapski, G.; Goldstein, S. *Proc. Natl. Acad. Sci. U.S.A.* **2000**, *97*, 8216.
- (15) Martinez, G. R.; Di Mascio, P.; Bonini, M. G.; Augusto, O.; Briviba, K.; Sies, H.; Maurer, P.; Rothlisberger, U.; Herold, S.; Kippenol, W. H. *Proc. Natl. Acad. Sci. U.S.A.* **2000**, *97*, 10307.

thermochemical and quantum mechanical calculations. Khan et al. reported formation of nitrosylhemoglobin through interaction of methemoglobin and peroxynitrite, suggesting that, upon protonation, peroxynitrite produced singlet oxygen and the nitroxyl anion that went on to react with methemoglobin. Other authors¹⁴ countered this argument, claiming instead that formation of NO₂ and OH radicals was thermodynamically favored, and that the observation of the nitrosyl complex was in error. Our experiments suggest that coordination of peroxynitrite by an oxidized metal center may indeed promote generation of oxo radicals and a reactive reduced nitro complex that can easily form a nitrosyl product, consistent with all of these observations.

Increased reactivity toward oxo transfer in the iron analogue FeTPP(NO₂) makes these compounds susceptible to disproportionation. Figures 3 and S1 show the apparent stability of the equilibrium mixtures of CoTPP(NO₂) with (py)CoTPP(NO₂) and (Cl₂py)CoTPP(NO₂) without excess pyridine ligand. The spectrum of the original equilibrium mixture in each figure was unchanged over a 2-week period. Addition of excess pyridine or dichloropyridine to the equilibrium mixtures after this period of time resulted in generation of the spectra attributable to the fully coordinated derivatives.

Conclusions

The similarity of structures and electrochemical behavior suggests that the hexacoordinate pyridine derivatives share a similar lack of reactivity toward oxo-transfer reactions, with differences attributable to the extent of the pyridine ligand dissociation. Oxidation strength increases substantially with removal of the pyridine ligand, although specificity of the oxo

transfer is lost with apparent generation of oxo radicals by way of the proposed peroxynitro complex intermediate that forms from reaction of dioxygen and the (nitrosyl)cobalt(II) porphyrin. Further study of this intermediate and its involvement in the overall oxo-transfer reactivity of the pentacoordinate cobalt(III) porphyrins is being pursued.

Acknowledgment. This work was funded in part by the Horry County Higher Education commission's support of Coastal Carolina University's Academic Enhancement Grants Program. Funding was also provided by the Southeast Regional Education Board for faculty (J.G.) travel to Clemson University, the South Carolina Governor's School for Science and Mathematics for support of high school research interns, and the Camille and Henry Dreyfus Foundation (W.P.) for support of the X-ray Crystallography workshop at Clemson University. Funding was also provided by the SC EPSCoR program for summer research support (V.E. and J.T.) and by the Cathcart Smith Foundation and the Department of Chemistry and Physics of Coastal Carolina University. Thanks are due to David Evans (CCU) for valuable conversations about organic reaction chemistry.

Supporting Information Available: Crystallographic data in CIF format. Cyclic voltammograms of (Me₂Npy)CoTPP(NO₂), (Cl₂py)-CoTPP(NO₂), and "CoTPP(NO₂)" prepared by adding LiClO₄ to the latter solution (Figures S1 and S2). Electronic spectra of (Cl₂py)CoTPP(NO₂) in CH₂Cl₂ under nitrogen after additions of solid Ph₃P (Figure S3). Electronic spectra of (Cl₂py)CoTPP(NO₂) in CH₂Cl₂ under nitrogen after addition of allyl bromide (Figure S4). Spectroscopic effects of the distal ligand (Table S1). This material is available free of charge via the Internet at <http://pubs.acs.org>.

IC001442E

(16) Kini, A. D.; Washington, J.; Kubiak, C. P.; Morimoto, B. H. *Inorg. Chem.* **1996**, *35*, 6904–6906.